Mutation Research - Genetic Toxicology and Environmental Mutagenesis 882 (2022) 503545

Contents lists available at ScienceDirect

Mutation Research - Genetic Toxicology and Environmental Mutagenesis

journal homepage: www.elsevier.com/locate/gentox

Lack of mutagenicity of TiO_2 nanoparticles *in vitro* despite cellular and nuclear uptake

Naouale El Yamani [a,1], Laura Rubio [b,1], Alba García-Rodríguez [b], Alena Kažimírová [c], Elise Rundén-Pran [a], Barančoková Magdalena [c], Ricard Marcos [b,*], Maria Dusinska [a,*]

[a] Health Effects Laboratory, Department for Environmental Chemistry, NILU – Norwegian Institute for Air Research, Kjeller, Norway
[b] Department of Genetics and Microbiology, Faculty of Biosciences, Universitat Autònoma de Barcelona, 08193 Cerdanyola del Vallès (Barcelona), Spain
[c] Department of Biology, Faculty of Medicine, Slovak Medical University, 833 03 Bratislava, Slovakia

ARTICLE INFO

Keywords:
Titanium dioxide nanoparticles NM-101
V79–4 and A549 cells
HPRT and comet assays, mutagenicity, cellular uptake, nuclear uptake

ABSTRACT

The potential genotoxicity of titanium dioxide (TiO_2) nanoparticles (NPs) is a conflictive topic because both positive and negative findings have been reported. To add clarity, we have carried out a study with two cell lines (V79–4 and A549) to evaluate the effects of TiO_2 NPs (NM-101), with a diameter ranging from 15 to 60 nm, at concentrations 1–75 μg/cm^2. Using two different dispersion procedures, cell uptake was determined by Transmission Electron Microscopy (TEM). Mutagenicity was evaluated using the *Hprt* gene mutation test, while genotoxicity was determined with the comet assay, detecting both DNA breaks and oxidized DNA bases (with formamidopyrimidine glycosylase - Fpg). Cell internalization, as determined by TEM, shows TiO_2 NM-101 in cytoplasmic vesicles, as well as close to and inside the nucleus. Such internalization did not depend on the state of agglomeration, nor the dispersion used. In spite of such internalization, no cytotoxicity was detected in V79–4 cells (relative growth activity and plating efficiency assays) or in A549 cells (AlamarBlue assay) after exposure lasting for 24 h. However, a significant decrease in the relative growth activity was detected at longer exposure times (48 and 72 h) and at the highest concentration 75 μg/cm^2. When the modified enzyme-linked alkaline comet assay was performed on A549 cells, although no significant induction of DNA damage was detected, a positive concentration-effects relationship was observed (Spearman's correlation = 0.9, p 0.0001). Furthermore, no significant increase of DNA oxidized purine bases was observed. When the frequency of *Hprt* gene mutants was determined in V79–4 cells, no increase was observed in the exposed cells, relative to the unexposed cultures. Our general conclusion is that, under our experimental conditions, TiO_2 NM-101 exposure does not exert mutagenic effects despite the evidence of NP uptake by V79–4 cells.

1. Introduction

The use and applications of nanoscale materials or nanoparticles (NPs) have exponentially expanded in different fields. NPs can display physicochemical properties (e.g. optical, magnetic, electrical, etc.) which make them particularly suitable in many sectors, such as medicine [1,2], textiles, agriculture, and cosmetics, as well as in the food industry and food packaging [3,4]. Due to their ability to confer opacity and whiteness, titanium dioxide (TiO_2) NPs are among the most used NPs in cosmetics as a UV filter and in the food industry as food additives [5,6]. TiO_2 NPs were authorized as a food additive (E171) in the EU according to Annex II of Regulation (EC) No 1333/2008. TiO_2 E171 contains at most 50% of particles in the nano range (i.e. less than 100 nm), to which consumers are daily exposed. Hence, concerns have been raised about its safety when included in cosmetics or in food as an additive. TiO_2 is considered as a non-soluble metal, and the potential mechanism of cytotoxicity induced by the non-soluble metal oxide NPs is a subject of current controversy [7]. Recently, and after conducting a review of all the relevant available scientific evidence related to the ingestion of TiO_2 NPs as food additive, the European Food Safety Authority (EFSA) published an updated opinion on safety of the TiO_2 NP food additive E171 where several studies on *in vitro* genotoxicity were included. The EFSA panel concluded that a concern for genotoxicity of TiO_2 NPs cannot be ruled out. Thus, TiO_2 NPs can no longer be

* Corresponding authors.
E-mail addresses: ricard.marcos@uab.cat (R. Marcos), maria.dusinska@nilu.no (M. Dusinska).
[1] Both persons contributed equally to the work

https://doi.org/10.1016/j.mrgentox.2022.503545
Received 26 July 2022; Received in revised form 29 August 2022; Accepted 30 August 2022
Available online 5 September 2022

considered as safe when used as a food additive [8]. This consideration was not related to other uses of TiO_2 NPs such as in cosmetics and biomedicine, which supports the need for further (geno)toxicological investigations using a wide variety of cell models [8]. On the other hand, the Health Canada Food Directorate has recently conducted its own comprehensive review of the available science and concluded the contrary. No health effect issues related the use of TiO_2 NPs as food additive were found, implying its safety [9]. The review pointed out that many of the studies raising concern about the safety of TiO_2 NPs, including the concern for genotoxicity, used forms of TiO_2 that are not considered acceptable for its use in food, and that have different properties from those of food-grade TiO_2. Consequently, further studies have been proposed [9]. The TiO_2 NP has also been evaluated by Scientific Committee for Consumer Safety (SCCS) for use in cosmetic products that lead to exposure by inhalation and was considered not safe [10]. TiO_2 is presently under evaluation by the Scientific Committee on Health, Environmental and Emerging Risks (SCHEER) for toys that include also TiO_2 NPs.

In vitro genotoxicity studies are important in the safety assessment of new compounds and products including NPs [11]. Genotoxicity is linked to several adverse outcomes including cancer [12]. From the regulatory perspective, genotoxicity testing requires a battery of tests addressing these different genotoxic and mutagenic endpoints, since no single method can detect all different forms of genome damage including DNA lesions, mutations, or chromosome aberrations [13–15]. Although there are many reports of potential genotoxic effects of TiO_2 NPs at the levels of both DNA damage (by the comet assay) and chromosome (micronucleus or chromosome aberration tests) [8], few studies have been conducted to investigate the ability of TiO_2 NPs to induce gene mutation. Therefore, we believe that providing mutagenicity data following OECD TG 476, and genotoxicity data obtained with the comet assay, is highly valuable in a weight-of-evidence evaluation for the human health risk assessment of TiO_2 NPs.

Gene mutations can either be point mutations or frameshift mutations where several base pairs can be affected [16]. The *in vitro* mammalian HPRT gene mutation test (OECD TG 476) is a conventional assays for gene mutation detection. The assay has been validated for use as a component of the genotoxic testing battery, which is used for evaluating the mutagenic/carcinogenic potential of chemicals. It has also been included in the testing battery for NP hazard assessment. The mammalian gene mutation assay is part of the risk assessment strategy for safety assessment of NPs as the Ames test is not suitable for testing NPs due to bacterial cell wall and size of bacteria [10,17].

As both positive and negative results have been obtained with TiO_2 NPs, our aim was to investigate mutagenicity and genotoxicity of one of the reference TiO_2 NPs from the European Commission Joint Research Center (JRC) repository (NM-101) with a diameter ranging from 15 to 60 nm, to add clarity to our present knowledge. We have selected the Chinese hamster lung fibroblast cells V79–4 as these cells are the recommended cell line by the OECD TG 476 and have a good uptake of nanomaterials [16]. To better understand the interaction of NPs with cellular matter and the observed effects, a confirmation of cellular uptake when testing NPs is a requirement.

In the present study, we assessed the mutagenic potential of (NM-101), employing different assays to better understand the mechanism of action. Moreover, we aimed to study whether the dispersion protocol interfered in the cell-NP interaction and outcomes. To study mutations induced by NPs, we used the V79–4 cells following the test guideline OECD 476 [18]. For the genotoxicity testing by the comet assay we used the human lung epithelial cell line (A549) as a representative and validated cell model for nanotoxicology studies [19–21]. With this cell line we have tested at least 50 NPs, among them eleven TiO_2 NPs, within several EU projects (FP6 NanoTEST, FP7 NANoREG, H2020, NanoREG2 and HISENT), and we have confirmed the suitability of this cell model to screen for early signs of genotoxicity [20–24].

2. Material and methods

2.1. Cell cultures

The V79–4 adherent cells isolated from the lung of a normal Chinese hamster (male), were purchased from the European Collection of Authenticated Cell Cultures (ECACC, catalogue number 86041102). Cells were cultured in Dulbecco's minimal essential medium (DMEM) D6046 (Sigma, Steinheim, Germany) supplemented with 10% (v/v) heat-inactivated fetal bovine serum (FBS, Gibco, Grand Island, NY, USA) and 1% (v/v) penicillin-streptomycin (Gibco) at 37 °C in a 5% CO_2 humidified atmosphere. Cells were thawed and sub-cultured 2–4 times before use in the experiments, at an initial density of 2×10^5 cells/mL in vented T-75 cm^2 flasks. The cells are used for cytotoxicity testing, by the RGA and PE assays, and for mutagenicity testing by the HPRT assay.

The human lung epithelial cell line A549 was kindly provided by GAIKER within the FP7 NANoREG project. Cells were cultivated in 75 cm^2 culture flasks in Dulbecco's modified Eagle medium (DMEM, Sigma) supplemented with 9% fetal bovine serum (FBS) and penicillin (100 U/mL) and streptomycin (100 μg/mL) and placed in a CO_2 incubator at 37 °C. Briefly, $1x10^4$ cells were seeded into each well of 96-well plates. The cells were seeded and exposed in duplicate to increasing concentrations of TiO_2 NM-101 for 3 or 24 h in a total volume of 200 μL per well. The cells are used for cytotoxicity testing by the AB assay and genotoxicity testing by the enzyme-modified comet assay.

2.2. Physicochemical characterization of nanoparticles

TiO_2 NPs NM-101, an anatase nanopowder of nominal size 21 nm (15–60 nm), were obtained from the Joint Research Centre (Ispra, Italy). NM-101 was well characterized under the frame of the NANOGENOTOX EU project showing primary particle size of approximately 6 nm in dimeter when measured by transmission electron microscopy (TEM) in its dry form and showing an agglomeration behaviour that formed clusters of 55 nm [22]. Despite previous characterization, further confirmation of size and size distribution using nanoparticle tracking analysis (NTA) were carried out after NPs dispersion. The hydrodynamic size and size distribution of the NPs dispersions were analysed in stock dispersion and in cell culture medium (before, during, and after the exposure) by NTA using a NanoSight NS500 (Malvern Panalytical), which enables measurement of the size of particles from about 30 nm to 1 μm. The instrument combines laser light scattering microscopy with a charge-coupled device (CCD) camera, which visualizes and records nanoparticles in dispersion. The hydrodynamic size was also measured using a DLS instrument and the sizes at 10 and 100 μg/mL are 152.2 ± 62.47 and 166.1 ± 12.55 respectively [22]. Other physicochemical properties were also investigated in the course of the NANoREG project and data on water solubility, PDI, zeta-potential are publically available via the EnanoMapper database and NANoREG results repository https://www.rivm.nl/en/international-projects/nanoreg.

Within the NANoREG project, the presence of endotoxin contamination of TiO_2 NM- 101 was investigated and reported in NANoREG results repository and NANoREG deliverable 5.06 [25]. The endotoxin contamination was assessed following a modified version of the LAL assay adapted to NPs. The presence of endotoxin in the TiO2 NM-101 core materials was considered low enough to allow further experimentation [25].

2.3. TiO_2 NM-101 dispersion and cell exposure

Two different dispersion protocols were followed. The TiO_2 NPs were dispersed either with or without the presence of serum in the stock solution. This allows investigation of whether the aggregation/agglomeration and stability of the dispersion could influence TiO_2 NPs observed effects.

2.3.1. Dispersion procedure 1 (DP1)

Stock suspensions of TiO_2 NPs at 5 mg/mL were freshly prepared for each experiment following the dispersion procedure DP1, developed as part of the FP7 project NanoTEST. Briefly, for 1 mL of stock suspension, 5 mg of TiO_2 NPs mixed with 1 mL of 10% foetal bovine serum (FBS, Gibco) in PBS (phosphate buffered saline) in a glass tube, was sonicated using an ultrasonic probe sonicator (Labsonic, Sartorius, Gottingen Germany) at 10% for 15 min

2.3.2. Dispersion procedure 2 (DP2)

The DP2 was developed under FP7 NANOGENOTOX project and adapted for the FP7 NANoREG project. A stock dispersion of 2.56 mg/mL was prepared as described by the NANOGENOTOX protocol [26]. Briefly, the TiO_2 NM-101 were first pre-wetted in 0.5% absolute ethanol and afterwards dispersed in Milli-Q water containing 0.05% bovine serum albumin (BSA). The obtained dispersion was sonicated using an ultrasonic probe sonicator (Labsonic P, 3 mm probe, from Sartorius Stedim Biotech, Göttingen, Germany) at 50% amplitude for 15 min on ice. The sonicator was previously calibrated, following the instructions provided by the NANOGENOTOX protocol to achieve an acoustic power of 7.35 ± 0.05 W [26].

From each resulting stock suspension, from each dispersion procedure, serial dilutions were made in cell culture medium to obtain the full range of NP suspensions, from (0.12–75 μg/cm^2, which were then immediately added to cells.

non-fluorescent whereas resorufin is red and highly fluorescent. The assay was performed as described in [20]. Briefly, after exposure of A549 cells to NPs (0.1–75 μg/cm^2) cells were washed with 1x PBS and incubated for 3 h with fresh culture medium supplemented with 10% AlamarBlue, after which 100 μL of medium from each well were transferred to a 96-well black polystyrene microplates (duplicate or triplicate aliquots). Fluorescence (excitation 530 nm, emission 590 nm) was measured on a FLUOstar OPTIMA microplate reader. The apparent viability (assessed as metabolic competence) was calculated as relative fluorescence intensity (FU) of the exposed samples devided by negative control * 100. cChlorpromazine (CHL), 50 μM was used as positive control. Due to the optical properties of TiO_2 NPs, controls for interference were also included. Briefly, cell-free wells were incubated with TiO_2 NP concentrations for the same time as cell exposure before fluorescence reading. The fluorescence readings are compared with the blank control samples (10% AB in cell culture medium without cells).

2.6. The proliferation assay - relative cell growth activity (RGA)

V79–4 cells were seeded on 12-well plates (1×10^5 cells per well) and incubated at 37 °C and 5% CO_2. After 24 h, cells were exposed to TiO_2 NPs for 24, 48, and 72 h at concentrations ranging from 0.12 to 75 μg/cm^2. At the end of the exposure period, medium was removed; cells were washed with 1x PBS, trypsinized and re-suspended in 1 mL medium. Ten μL of the cell suspension was mixed with 10 μL 0.4% trypan blue (Invitrogen) and the percentages of living cells (unstained) and stained cells with damaged membranes were measured using a Countess™ Automated Cell Counter (Invitrogen). Measurements were performed immediately upon staining (for all three exposure times).

$$RGA\% = \frac{\left(\frac{number\ of\ living\ cells\ at\ day\ n}{number\ of\ seeded\ cells\ at\ day\ 0}\right) in\ exposed\ cultures}{\left(\frac{number\ of\ living\ cells\ at\ day\ n}{number\ of\ seeded\ cells\ at\ day\ 0}\right) in\ unexposed\ control\ cultures} \ x\ 100$$

2.4. Cellular uptake measurement by transmission electron microscopy (TEM)

Cellular uptake of TiO_2 NPs was measured by TEM on the V79–4 cells. The cells were grown on 6-well plates at a density of 1.75×10^5 cells/well. Cells were exposed to TiO_2 NPs dispersed according to DP1 and DP2 (3, 10, 30 μg/cm^2) for 24 h. At the end of the exposure time, cells were washed twice with 1x PBS, trypsinized with 1% trypsin-EDTA, collected in a 15 mL tube and centrifuged for 8 min at 1000 rpm. The cell pellet was fixed in 2.5% (v/v) glutaraldehyde (EM grade, Merck, Darmstadt, Germany) and 2% (w/v) paraformaldehyde (EMS, Hatfield, PA, USA) in 0.1 M cacodylate buffer at pH 7.4 (PB, Sigma-Aldrich, Steinheim, Germany), and processed following conventional procedures, as previously described [22]. Samples were first post-fixed with osmium tetroxide, dehydrated in acetone, embedded in Epon, and finally polymerized at 60 °C, and cut with an ultramicrotome Leica EM UC6 using a diamond knife and mounted on copper grids. Before image acquisition, ultra-fine sections were stained using uranyl acetate and Reynolds lead-citrate solutions. All images were examined using a JEOL 1400 (JEOL LTC, Tokyo, Japan) TEM at 120 kV equipped with a CCD GATAN ES1000W Erlangshen camera.

2.5. The AlamarBlue assay

AlamarBlue (AB) measures cytotoxicity through a colorimetric response to the intracellular reducing metabolism of living cells. The conversion of resazurin (oxidised form) to resorufin (reduced form) results in colorimetric and fluorescence changes; resazurin is blue and

Methyl methane sulfonate (MMS), 100 μM was used as positive control. RGA was calculated according to the following formula:

2.7. The plating efficiency assay (PE)

The plating efficiency assay using the V79–4 cells was conducted in parallel with the gene mutation assay. The cells were exposed to TiO_2 NPs for 24 h, washed and counted as described for the RGA assay. Then, 50 cells per well were inoculated in 6-well plates (1 plate for each concentration tested) and left in an incubator at 37 °C for 10 days. The cells were then stained with 1% methylene blue (Sigma) and the number of colonies was counted manually. MMS, 100 μM was used as positive control. PE was calculated according to the following formula:

$$PE = \frac{number\ of\ colonies\ in\ exposed\ cultures}{number\ of\ colonies\ in\ unexposed\ cultures} \ x\ 100\ \%$$

2.8. DNA damage measured by the standard alkaline and enzyme-modified mini-gel comet assay

The alkaline enzyme-linked version of the comet assay was performed as described [20,27]. Briefly, A549 cells were seeded in 96-well plates (1×10^4 cells /well) for 24 h before exposure. On the day of the exposure, the cells were exposed to freshly dispersed TiO_2 NPs for 3 or 24 h. Depending on results of cytotoxicity tests, the highest concentrations were in some cases omitted. At the end of exposure, cells were washed with 1x PBS, trypsinised and re-suspended in medium.

Approximately 0.5 x 10^4 cells were transferred to a 96-well plate and mixed with low melting point (LMP) agarose (0.8% in PBS) at 37 °C. Drops of 10 μL were placed on previously pre-coated glass slides (0.5% normal melting point agarose). In our set-up, we used the format of 12-gels per slide, with 2 gels per concentration. After 5 min at 4 °C, the slides were immersed into cold lysis solution (2.5 M NaCl, 0.1 M EDTA, 10 mM Tris, 10% Triton X-100, pH 10) and incubated overnight. After lysis, slides were placed in cold alkaline solution (0.3 M NaOH, 1 mM EDTA, pH>12) and incubated for 20 min, followed by electrophoresis at 1.25 V/cm for 20 min in a horizontal electrophoresis tank. Slides were then washed twice in PBS followed by water and allowed to dry.

For visualization, the gels were stained with SYBRGold® (Invitrogen) diluted at 1 μL/mL in Tris-EDTA buffer (10 mM Tris–HCl, 1 mM Na_2-EDTA, pH 7.5–8), covered with a coverslip and examined under a fluorescence microscope (Leica DMI 6000 B). Images of comets were scored using the Comet Assay IV software (Perceptive Instruments), calculating the median percentage of DNA in the tail from 50 comets per gel, as a measure of DNA strand breaks (SBs).

For DNA base oxidation detection, a modified version of the comet assay protocol was applied by inclusion of a post-lysis incubation with DNA-formamidopyrimidine glycosylase (Fpg) that converts oxidized purines to strand breaks. After lysis, the slides were washed twice with Fpg buffer (40 mM HEPES, 0.1 M KCl, 0.5 mM EDTA, 0.2 mg/mL BSA, pH 8.0) before incubation for 30 min at 37 °C in a humidified box with Fpg diluted in the Fpg-buffer. At the end of the enzyme incubation, the slides were transferred into alkaline electrophoresis buffer and processed from this point as described above. NetFpg sites were calculated as the difference between % DNA in tail plus Fpg and % DNA in tail without Fpg.

All experiments included positive and negative controls. As positive control for SBs, cells were treated with H_2O_2 (100 μM in PBS), for 5 min at 4 °C. For the DNA oxidized bases, cells were treated with the photosensitizer Ro19–8022 (Hoffmann La Roche) at 2 μM in 1x PBS and irradiated with visible light (500 W halogen source, 30 cm from cells) for 5 min on ice. Additional controls to check for possible TiO_2 NP interference with the assay were made. Briefly the highest concentration of TiO_2 NPs to be tested was mixed with the cells from the negative control directly before embedding with agarose (no incubation or treatment). All slides were handled in parallel to the other slides as described above. To calculate the net Fpg-sensitive sites, the % of DNA in tail (without enzyme) was subtracted from the % of DNA in tail (with Fpg).

2.9. The Hprt gene mutation assay using V79-4 cells (TG 476)

The mammalian *in vitro* HPRT gene mutation test was carried out according to OECD test guideline TG 476 [18]. The day before exposure, the V79–4 cells were seeded on 6-well plates (1×10^5 cells per well) and incubated at 37 °C and 5% CO_2. After 24 h, the cells were exposed to TiO_2 NPs for 24 h, at concentrations 0.12, 0.6, 3, 15, and 75 μg/cm^2. At the end of the exposure, the cell culture medium was removed, cells were washed, trypsinized and re-suspended in 2 mL medium. The cells were seeded back in ϕ100 mm Petri dishes (3×10^5 cells/Petri dish, 3 dishes per sample to achieve approximately 10^6 cells per sample) and grown in complete culture medium for an additional 8 days. For cells to develop mutants, they were harvested twice in ϕ100 mm Petri dishes at days 6 and 8 in a selective medium containing 6-thioguanine (5 μg/mL, Sigma). The cells were then incubated for a further 10 days to allow formation of colonies. At the end of the incubation time, the mutant colonies were stained with 1% methylene blue and counted manually. Only colonies with a minimum of 50 cells were considered. The cell survival was assessed by the PE assay which was conducted in parallel as described in previous section 2.7. The viability of cells was determined at the time of each mutant harvest and calculated based on the number of colonies versus the number of inoculated cells. MMS (0.1 mM; 3 h) (Sigma) was used as positive control.

Mutant frequency was calculated according to the following formula:

$$Mutant\ \ frequency\ \ \left(x10^6\right) = \frac{number\ \ of\ \ mutant\ \ colonies}{number\ \ of\ \ colonies\ \ from\ \ untreated\ \ cells}$$

2.10. Statistical analysis

For data normality we used D'Agostino-Pearson normality test and Shapiro-Wilk test. The comet assay, PE and mammalian gene mutation data passed the normality test without log-transformation. The AlamarBlue and RGA data sets passed the normality test after log-transformation. The one-way analysis of variance ANOVA test was used, followed by Dunnett's multiple comparison test for the post hoc analysis. A correlation analysis of the genotoxic effects of the TiO_2 NPs as a function of exposure concentration and effect (Pearson's correlation) was performed, followed by a linear regression analysis. Prism 9.0 (GraphPad Software, San Diego, CA, USA) and Microsoft Excel 2013 were used for statistics and mathematical analysis. Differences with $p < 0.05$ were considered statistically significant.

3. Results

3.1. TiO_2 NM-101 characterization

Several physicochemical properties related to the primary properties of the NM-101 NPs were collected. The characterization was carried out in the frame of the EU-FP7 NANOGENOTX and NANoREG projects. To fulfil the requirements of the project and also follow ECHA recommendations when testing NPs [28], the secondary characterization (in medium) was also conducted in dispersion stock as well as in cell culture medium at times 0, 3, and 24 h using NTA (Nanosight, Malvern Panalytical) (Table 1). The size of NM-101 increased in the cell culture medium (DMEM) immediately after TiO_2 NPs was dispersed. Aggregation was also seen in cell culture medium at 3 and 24 h measurement compared with the stock dispersion.

Table 1
Physicochemical parameters of the TiO_2 NM-101. The listed analytical data were mainly generated by the EAHC NANOGENOTOX project, the EU FP7 project ENPRA, or retrieved from the (JRC) data-reports on OECD WPMNM.

Primary characterisation			
Material Code	NM-101	Shape (1-spherical, 2-rod)	1
Class	TiO_2	BET[3]_SSA[4] (m2/g)	316
"Core material"	TiO_2	TGA[5] (heating) Mass loss [wt%]	8
Polymorph	anatase	Catalyst/Impurity [wt%]	0.4
Product type	powder	associated inorganic/coating	no
XRD[1] size [nm]	6.9 ± 5.9	Organic coat/ associated organics	silanes, hexadecanoic and oxydecanoic acids
TEM[2] diameter (nm)	6.0 ± 0.7	Aggregated (TEM/ SEM)	yes
Secondary characterisation (DP1) by NTA			
Size (nm) (Stock, 0 h)	106.0 ± 8	Size (nm) (DMEM, 3 h)	237.0 ± 96.0
Size (nm) (DMEM, 0 h)	121.0 ± 9	Size (nm) (DMEM, 24 h)	167.0 ± 39.4
Secondary characterisation (DP2) by NTA			
Size (nm) (Stock, 0 h)	189.0 ± 53.1	Size (nm) (DMEM, 3 h)	231.7 ± 5.0
Size (nm) (DMEM, 0 h)	175.5 ± 38.8	Size (nm) (DMEM, 24 h)	182.0 ± 76.7

[1]XRD, X-ray diffraction; [2]TEM, Transmission electron microscope; [3]BET, Brunauer, Emmet and Teller (for the measurement of the specific surface NTA-Nanoparticle tracking Analysis

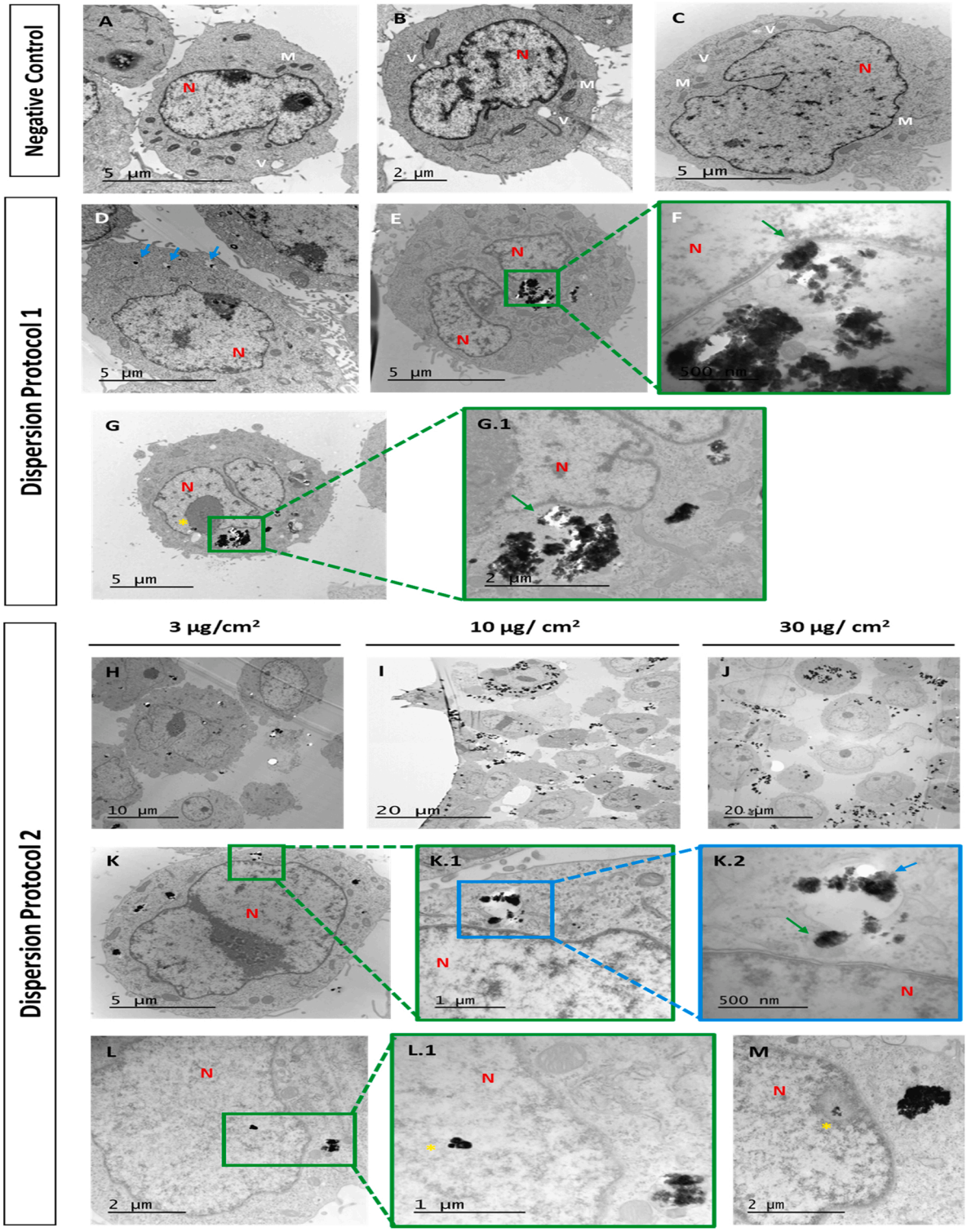

Fig 1. Representative TEM images after V79–4 Chinese hamster lung fibroblasts were exposed to 3, 10, and 30 µg/cm^2 TiO_2 NPs for 24 h. Untreated cells represented as negative control (A-C). V79–4 cells exposed to TiO_2 NPs dispersed using protocol 1 (D-G.1). V79–4 cells exposed to TiO_2 NPs dispersed using protocol 2 (H-M). N = nucleus; V = empty vesicles, M = mitochondria. Yellow asterisks indicate TiO_2 NPs inside cell nuclei; green arrow indicates TiO_2 NPs close or in direct contact with the nuclei membrane; and blue arrow indicate vesicles containing TiO_2 NPs. (For interpretation of the references to colour in this figure legend, the reader is referred to the web version of this article.)

3.2. V79-4 cellular uptake and sub-cellular localization

The potential cellular uptake and subcellular localization of the TiO_2 NM-101 in V79–4 cells was investigated and confirmed by TEM after exposures to 3, 10, and 30 µg/cm^2, dispersed according to both DP1 and DP2 procedures (Fig 1). TEM images confirmed that after 24 h exposure, the TiO_2 NPs were clearly taken up by V79–4 cells independently of the dispersion protocol used and the concentration applied. The TEM images show that TiO_2 was mostly aggregated. After 24 h exposure, the TiO_2 NP aggregates are observed outside the cells attached to the

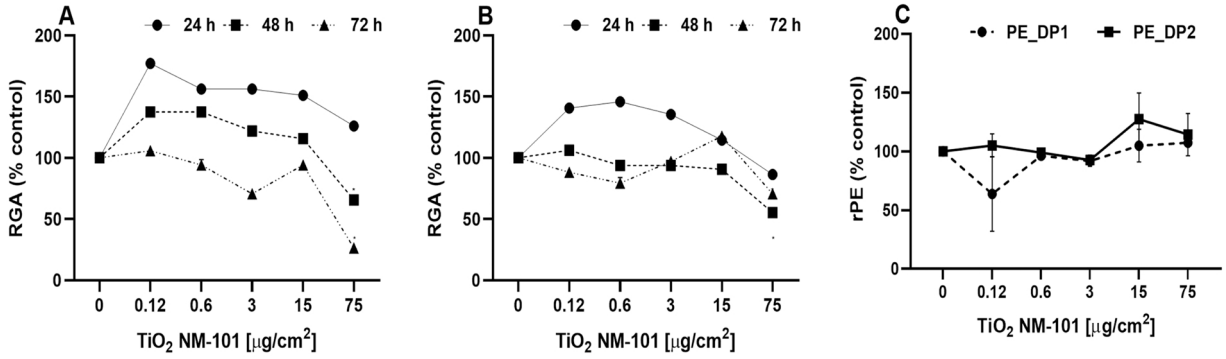

Fig 2. Cytotoxic effects of NM-101 on V79–4 cells after exposure to different concentrations of NM-101 measured as relative growth activity (RGA) (A & B) and plating efficiency (PE) (C). The RGA experiments were carried out after 24, 48, and 72 h of exposure to TiO2 NPs (DP1) (A) and exposure to TiO_2 NPs (DP2) (B) where cell number was counted in each time point immediately following staining. For the PE assay (C), immediately after the exposure TiO_2 NPs, 50 cells per dish were inoculated and the number of cell clones was calculated after 10 days of incubation. Data represent cytotoxicity relative to 100% of control and are expressed as mean ± SD of two independent experiments. *a statistically significant ($p < 0.05$) difference from the unexposed (control) cells. DP1 – dispersion protocol 1; DP2-dispersion protocol 2.

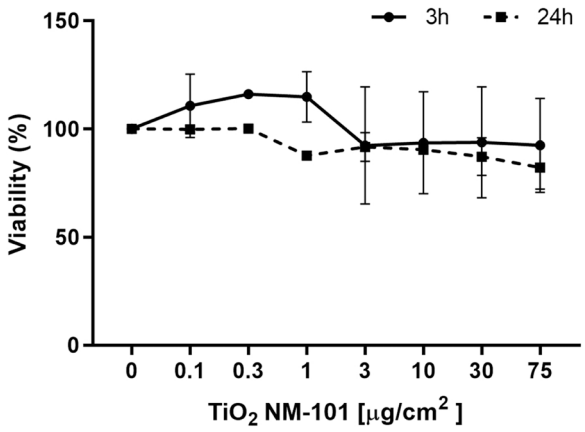

Fig 3. Cell viability measured as fluorescence intensity (%) after metabolic fluorescence activation in viable cells by the AlamarBlue assay after exposure of A549 cells to TiO_2 NM-101 (DP2) for 3 or 24 h. The results are shown as the mean ± SD from three independent experiments. For each experiment, exposure was performed in duplicates and from each well three replicate wells for reading of fluorescence were applied. Cell viability is presented as relative to negative control, set to 100%. h, hours; SD, standard deviation.

cellular membrane, inside the cell cytoplasm near the membrane (inside cytoplasmic vesicles, vacuoles, endosomes, or lysosomes like structures), or attached to the nuclear membrane, as well as inside the nucleus (Fig 1, L-M).

3.3. Cytotoxicity testing by the RGA, PE, and AlamarBlue assays

The cytotoxicity of NM-101 was measured by RGA% and PE% on V79–4 cells and by the colorimetric assay AlamarBlue on A549 cells. The RGA% was determined as the ratio of the number of living cells at 24, 48, and 72 h in exposed versus unexposed cultures (Fig 2A). The PE% was determined as the ratio of the number of colonies in exposed cultures versus unexposed (Fig 2B). TiO_2 NPs were found to be non-cytotoxic by both RGA and PE assays in V79–4 cells (Fig 2). These results were similar to the observed effect on A549 cells using the AB assay after exposures lasting for both 3 or 24 h (Fig 3). However, TiO_2 NPs exposure in the RGA assay lasting for 72 h caused a significant decrease of the RGA%, compared to untreated cells (Fig 2A). Treatment with CHL (for AlamarBlue) and MMS (for RGA and PE) resulted in significant positive effects (data not shown).

3.4. Genotoxicity testing measured by the standard alkaline and enzyme-modified mini-gel comet assay

The genotoxic potential of NM-101 was measured on A549 cells by a miniaturised version of the alkaline comet assay. Only concentrations consistent with below or equal to 60% viability were considered for evaluation of genotoxicity, to distinguish between true DNA damage and secondary damage due to cell death. DNA SBs and DNA oxidised bases (net Fpg sites) were measured as DNA tail intensity (%). The NM-101 did not exhibit any significant increase on DNA SBs (due to the high dispersion of the data) or oxidised bases after 3 or 24 h, but we found positive concentration-response relationship for SBs (Peasrson's correlation= 0.85, $p < 0.001$) (Fig 4A).

3.5. Mutagenic effect of NM-101 measured by the Hprt gene mutation assay using V79-4 cells

In our study we assessed the potential mutagenicity of TiO_2 NM-101 in V79–4 cells in two independent parallel experiments and at two harvest time points. TiO_2 dispersed according to both DP1 and DP2 protocols was tested. The positive control MMS (0.1 mM for 3 h) induced a clear increase of *Hprt* mutant frequencies 76.02 ± 19.24 per ($x10^6$ viable cells) that was significantly different form the negative control. The exposure to TiO_2 NM-101 at all tested concentrations 3, 15, and 75 μg/cm^2 did not induce any statistically significant increase in mutants frequency in V79–4 cells compared to the untreated cells. The lack of mutagenic effects was independent of the dispersion protocol followed (Fig 5).

4. Discussion

The safety of TiO_2 NPs has been questioned on several occasions, and many genotoxicity studies have been conducted, but with conflicting results [29]. According to extensive EFSA evaluation [8], the use of TiO_2 NPs (E171) as food additive is not safe due to uncertainty and mode of action involved (threshold or non-threshold). Additionally, SCCS, in an opinion on the use of TiO_2 NPs for use in cosmetic products that lead to exposure by inhalation, also considered TiO_2 NP not safe [30].

In our study, we tested one JRC TiO_2 NP (NM101, an anatase form known to be hardly soluble or even insoluble). We have used a battery of assays covering a range of endpoints: cytotoxicity (RGA, PE, and AB assays), genotoxicity for DNA damage (both SBs and oxidized bases by the comet assay), and gene mutation by using the *Hprt* assay. We have also tested TiO_2 NPs dispersed by following two different methods. The two dispersion methods seemed not to differ from each other when

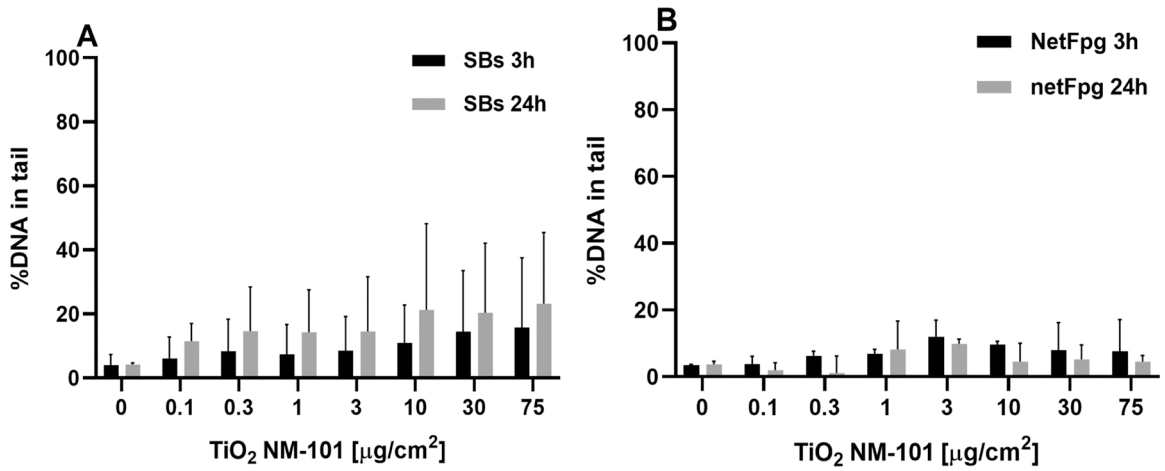

Fig 4. DNA strand breaks (SBs) measured by the standard alkaline comet assay (A) and oxidised purine bases (B) measured by the enzyme (formamidopyrimidine glycosylase – Fpg) modified comet assay in A549 cells after the exposure to TiO_2 NM-101 (DP2) for 3 or 24 h. The effect is expressed as tail intensity (%). Three independent experiments were performed with duplicate wells for each exposure. The results are shown as mean of the median of duplicate wells from each of the three experiments ± SD. h, hours; SD, standard deviation. Net Fpg sites, was estimated as Fpg sensitive sites detected after Fpg incubation minus SBs (no enzyme incubation). Hydrogen peroxide (100 μM, 5 min in PBS), a positive control for SBs gave 64.63% DNA in tail, Ro-198022 photosentizer with UV light (2 μM) a positive control for oxidised DNA lesions (netFpg) gave 51.02% of DNA in the tail.

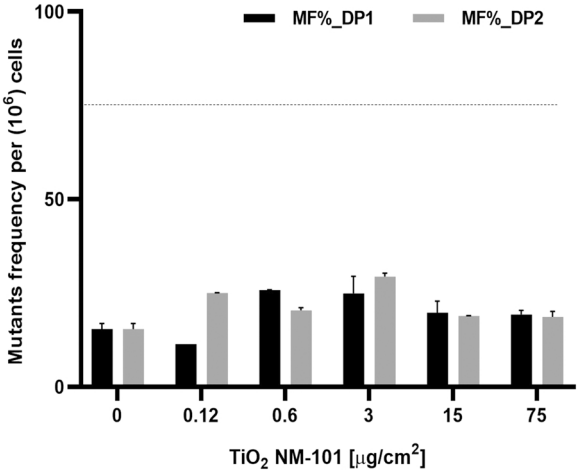

Fig 5. Induction of *Hprt* gene mutants after the exposure of V79–4 cells to different concentrations of TiO_2 NPs for 24 h. The mutant frequencies per 10^6 viable cells (MF%) are expressed as the mean±SD of two independent harvests. SD, standard deviation; DP1, dispersion protocol 1; DP2, dispersion protocol 2; h, hours. Mutant frequency in cells treated with the positive control methylmethane sulfonate (MMS, 100 mM) gave 76 per 10^6 *Hprt* gene mutants per 10^6 viable cells. This value is indicated as a dotted line. Dunnett test * * $p < 0.1$, * ** $p < 0.01$.

comparing toxicity measured by the RGA and PE assays, nor by their mutagenic effect in the *Hprt* assay. Our results show that TiO_2 NPs were non-cytotoxic in the RGA and PE assays using V79–4 cells, nor in the AlamarBlue assay in A549 cells, which agrees with the work published by Garcia-Rodriguez *et al.,* where the same TiO_2 NPs were tested after 24 h exposure using two lung-model cells (A549 and Beas-2B) [22]. A non-cytotoxic effect was also obtained after exposure of V79 cells to NM-101 using the MTT assay (NANoREG Deliverable 5.06, Page 80 of 105). However, exposures lasting for 48 and 72 h caused a significant decrease in the RGA%. Thus, there is a concentration and time-dependent effect of exposures lasting up to 72 h, as previously described [31]. There are many studies showing DNA-damaging effects of TiO_2 NPs [20, 21, 32–34]. In another study, six TiO_2 NPs with different physicochemical properties were tested under the same experimental conditions using the modified comet assay and the outcomes on DNA damage (both SBs and oxidized lesions) were different, NM-101 giving equivocal results and NM-100 being the most genotoxic [21]. In the present study of TiO2 NM-101 with the comet assay, there was no significant increase in SBs compared to the negative control (due to the high variability of the obtained data) nor in oxidised bases (Fpg sites), but a positive concentration-response relationship was seen for SBs. In the study by Rodriguez et al., equivocal data on SBs and no oxidative damage were observed in both A549 and Beas2B, Beas2B cells being less sensitive than A549 [22]. A study in BEAS-2B showed that the effects of TiO_2 were associated with the shape and only those forms that were clearly internalized into cells (food grade, P25, and platelets) were able to induce genotoxicity [35].

It is well accepted that the cellular toxicity of NPs is strictly related to their physicochemical properties such as size, shape, stability, mode of synthesis, and surface chemistry [23, 36–38] and depends also on their uptake by cells [39]. Once endocytosed, slightly soluble or insoluble nanoparticles could either accumulate in the acidic endo-lysosomal organelles or leave the cell by exocytosis [40]. In addition to NPs' crystallinity and solubility properties, particle size is an important factor for determining toxicity. It has been shown that big NPs (or agglomerated particles) dissolve more slowly than small sized particles [41]. This is mainly due to the endocytosis phenomenon which is size dependent [40, 42]. The cellular uptake was found to be kinetically activated and strongly dependent on agglomeration state and not on the primary particle size. It is important to consider the role of the proteins present in the culture medium that can join to the NPs forming a corona that can modulate the uptake efficiency [43–45]. According to our NTA and TEM analysis, TiO_2 NP size increased after dispersion in cell culture medium, by both dispersion methods, and the NPs were present in the cells mainly in the form of aggregates/agglomerates. Also, Jalili et al., (2022) observed accumulation of very large aggregates occupying the cytoplasm of Caco2 and HepaRG cells after both chronic and long-term exposure to the JRC rutile TiO_2 NM-103 and NM-104. They also observed that after a week of recovery (after 24 h exposure), the TiO_2 NPs were still present inside the cells [46].

In our study, we found TiO_2 NPs attached to the cellular membrane, inside the cell in cytoplasmic vesicles near the membrane, in vacuoles, endosomes, or lysosome-like structures that were in close proximity to the nuclear envelope, attached to the nuclear membrane, as well as inside the nucleus. Other studies on TiO_2 NPs also showed the presence of

TiO_2 NPs in the nucleus either as single particles or as agglomerates [47–53]. Ahlinder et al. (2013) demonstrated nuclear uptake by two techniques – TEM and Raman spectroscopy. In addition, TiO_2 NPs were identified in the nuclei closely associated with the phosphorus-positive chromatin signal [52]. This indicates that the cells may use different mechanisms and molecular pathways of NPs internalization. One of the main mechanisms of cellular uptake is endocytosis [46]. According to our TEM images, we could consider both pinocytosis as well as phagocytosis as the mechanisms involved in the uptake. We observed highly ruffled regions of the cell membrane forming a pocket which then is released in the form of a vesicle with the aggregated TiO_2 NPs inside. The cell membrane also creates pseudopodia or extensions of the cell membrane surrounding the aggregates before forming a phagocyte vesicle. Just beneath the plasma membrane we could also see early and late endosomes, as well as lysosome-like endosomes near the nucleus. TiO_2 NPs may be transported to the cell nucleus through nuclear pores by passive diffusion, or by interaction with transport receptors [54,55]. How aggregates of NPs appear inside the nucleus is largely unknown. One possibility is that the process takes place during cell division [56]. Here we speculate that also fusion of nuclear membrane with a vesicle containing aggregates of TiO_2 NPs could take place but to prove this further investigations are needed. Although the presence of TiO_2 NPs inside the nucleus would suggest a potential source of DNA damage, only a concentration-response relationship in SBs and no DNA base oxidation were observed by the comet assay. No induction of gene mutation was observed when the presence of mutants in the *Hprt* gene was evaluated. It is important to indicate that, so far, only a few studies have been conducted on the mutagenic effect of TiO_2 NPs, and most of them reported negative results. The negative effects on the gene mutation assay in our study are similar to those reported previously by other authors using the HPRT assay with V79–4 cells [53,57], or the mouse lymphoma assay [58]. Only two studies reported a positive effect using the HPRT assay in V79 cells after exposure lasting for only 2 h to one anatase TiO_2 [51,59].

To sum up, many studies reported positive DNA damaging and clastogenic effects of TiO_2 NPs [8,32,60] although some negative results were also reported [8,61,62]. We assume that the reasons for the different results among the various studies maybe related to different TiO_2 NP species, experimental conditions and set up, or small variation in laboratory routines that may influence physicochemical properties of NPs before and during the treatment. Contradictory results are also typical for example for relatively week mutagens or compounds that can easily change their properties.

Genotoxic damage has often been attributed to the generation of reactive oxygen species (ROS) [63,64]. Induction of ROS by NM-101 was investigated within NANoREG project and no ROS production was observed compared to the positive control [25].

We can speculate that though generally the main mechanism of NPs genotoxicity is mostly indirect (through oxidative stress), direct mechanism of genotoxicity is also possible, as we found TiO_2 NP agglomerates also in the nucleus. It is expected that larger agglomerates can destroy/damage chromosomal (DNA) structures rather than causing gene mutations.

Our results are in concordance with the recent EFSA evaluation that TiO_2 NPs could have the potential to induce DNA strand breaks and chromosomal damage, but not gene mutations.

5. Conclusion

As a conclusion of our studies, negative gene mutation results (*Hprt* mutation test) were obtained. Additionally, no significant increase in DNA SBs, with only a concentration-response relationship, and no oxidized DNA bases (measured by the comet assay) were found after exposure to TiO_2 NPs. It is important to point out that negative mutagenicity was found even though efficient cellular uptake of TiO_2 NPs was demonstrated. Importantly, such cellular uptake is not only confined to the cytoplasm, since TiO_2 NPs are also observed inside the nucleus.

Funding

This work was supported by the EC FP7 NANoREG [grant agreement NMP4-LA-2013–310584]; the Research Council of Norway, project NorNANoREG [239199/O70]; the European Union's Horizon 2020 research and innovation program projects NanoREG2 [grant agreement 646221]; RiskGONE [grant agreement 814425]; NanosolveIT [grant agreement 814572]; VISION [grant agreement 857381], TWINALT [grant agreement 952404] and CompSafeNANO [grant agreement 101008099]. A. García-Rodríguez received funding from the post-doctoral fellowships programme Beatriu de Pinós, funded by the Secretary of Universities and Research [Government of Catalonia] and by the Horizon 2020 programme of research and innovation of the European Union under the Marie Sktodowsdka-Curie grant agreement No 801370. L. Rubio was supported by a contract Juan de la Cierva [IJC2020–2686I/AEI/10.13039/501100011033].

Declaration of Competing Interest

The authors declare that they have no known competing financial interests or personal relationships that could have appeared to influence the work reported in this paper.

References

[1] J.T. Seil, T.J. Webster, Antimicrobial applications of nanotechnology: methods and literature, Int. J. Nanomed. 7 (2012) 2767–2781.
[2] A. Mahapatro, D.K. Singh, Biodegradable nanoparticles are excellent vehicle for site directed in-vivo delivery of drugs and vaccines, J. Nanobiotechnol. 9 (2011) 1–11.
[3] N. Barkalina, C. Charalambous, C. Jones, K. Coward, Nanotechnology in reproductive medicine: emerging applications of nanomaterials, Nanomed.: Nanotechnol., Biol., Med. 10 (2014) 921–938.
[4] A. Grobe, M.E. Rissanen, Nanotechnologies in agriculture and food - an overview of different fields of application, risk assessment and public perception, Recent Pat. Food, Nutr. Agric. 4 (2012) 176–186.
[5] Z.F. Yin, L. Wu, H.G. Yang, Y.H. Su, Recent progress in biomedical applications of titanium dioxide, Physical chemistry chemical physics, PCCP 15 (2013) 4844–4858.
[6] A. Weir, P. Westerhoff, L. Fabricius, K. Hristovski, N. von Goetz, Titanium dioxide nanoparticles in food and personal care products, Environ. Sci. Technol. 46 (2012) 2242–2250.
[7] J. Khalili Fard, S. Jafari, M.A. Eghbal, A review of molecular mechanisms involved in toxicity of nanoparticles, Adv. Pharm. Bull. 5 (2015) 447–454.
[8] Safety EFSA, assessment of titanium dioxide (E171) as a food additive, EFSA J. 19 (2021), e06585.
[9] Health-Canada, Health Canada report on TiO2, (2022).
[10] SCCS, Guidance on the safety assessemnt of nanomaterials in cosmetics, 2019.
[11] H. Cowie, Z. Magdolenova, M. Saunders, M. Drlickova, S. Correia Carreira, B. Halamoda Kenzaoi, L. Gombau, R. Guadagnini, Y. Lorenzo, L. Walker, L. M. Fjellsbo, A. Huk, A. Rinna, L. Tran, K. Volkovova, S. Boland, L. Juillerat-Jeanneret, F. Marano, A.R. Collins, M. Dusinska, Suitability of human and mammalian cells of different origin for the assessment of genotoxicity of metal and polymeric engineered nanoparticles, Nanotoxicology 9 (Suppl 1) (2015) 57–65.
[12] M. Carbone, S.T. Arron, B. Beutler, A. Bononi, W. Cavenee, J.E. Cleaver, C. M. Croce, A. D'Andrea, W.D. Foulkes, G. Gaudino, J.L. Groden, E.P. Henske, I. D. Hickson, P.M. Hwang, R.D. Kolodner, T.W. Mak, D. Malkin, R.J. Monnat Jr., F. Novelli, H.I. Pass, J.H. Petrini, L.S. Schmidt, H. Yang, Tumour predisposition and cancer syndromes as models to study gene-environment interactions, Nat. Rev. Cancer 20 (2020) 533–549.
[13] M. Dusinska, E. Mariussen, E. Runden-Pran, A.M. Hudecova, E. Elje, A. Kazimirova, N. El Yamani, N. Dommershausen, J. Tharmann, D. Fieblinger, F. Herzberg, A. Luch, A. Haase, In vitro approaches for assessing the genotoxicity of nanomaterials, Methods Mol. Biol. 1894 (2019) 83–122.
[14] M. Dusinska, J. Tulinska, N. El Yamani, M. Kuricova, A. Liskova, E. Rollerova, E. Rundén-Pran, B. Smolkova, Immunotoxicity, genotoxicity and epigenetic toxicity of nanomaterials: new strategies for toxicity testing? Food Chem. Toxicol.: Int. J. Publ. Br. Ind. Biol. Res. Assoc. 109 (2017) 797–811.
[15] S.H. Doak, B. Manshian, G.J. Jenkins, N. Singh, In vitro genotoxicity testing strategy for nanomaterials and the adaptation of current OECD guidelines, Mutat. Res. 745 (2012) 104–111.
[16] R.K. Shukla, A. Badiye, K. Vajpayee, N. Kapoor, Genotoxic potential of nanoparticles: structural and functional modifications in DNA, Front. Genet. 12 (2021).
[17] S. EFSA, V. More, D. Bampidis, C. Benford, T. Bragard, A. Halldorsson, S. Hernández-Jerez, K. Hougaard Bennekou, C. Koutsoumanis, K. Lambré,

H. Machera, S. Naegeli, J. Nielsen, D. Schlatter, V. Schrenk, D. Silano, M. Turck, J. Younes, Q. Castenmiller, F. Chaudhry, R. Cubadda, D. Franz, J. Gott, A. Mast, A. G. Mortensen, S. Oomen, E. Weigel, A. Barthelemy, J. Rincon, R. Tarazona, Schoonjans, Guidance on risk assessment of nanomaterials to be applied in the food and feed chain: human and animal health, EFSA J. 19 (2021), e06768.

[18] OECD, Test No. 476: In Vitro Mammalian Cell Gene Mutation Tests using the Hprt and xprt genes, 2016.

[19] A. Huk, E. Izak-Nau, N. El Yamani, H. Uggerud, M. Vadset, B. Zasonska, A. Duschl, M. Dusinska, Impact of nanosilver on various DNA lesions and HPRT gene mutations - effects of charge and surface coating, Part. Fibre Toxicol. 12 (2015) 25.

[20] N. El Yamani, A.R. Collins, E. Rundén-Pran, L.M. Fjellsbø, S. Shaposhnikov, S. Zienolddiny, M. Dusinska, In vitro genotoxicity testing of four reference metal nanomaterials, titanium dioxide, zinc oxide, cerium oxide and silver: towards reliable hazard assessment, Mutagenesis 32 (2017) 117–126.

[21] N. El Yamani, E. Mariussen, M. Gromelski, E. Wyrzykowska, D. Grabarek, T. Puzyn, S. Tanasescu, M. Dusinska, E. Rundén-Pran, Hazard identification of nanomaterials: in silico unraveling of descriptors for cytotoxicity and genotoxicity, Nano Today 46 (2022), 101581.

[22] A. Garcia-Rodriguez, L. Rubio, L. Vila, N. Xamena, A. Velazquez, R. Marcos, A. Hernandez, The Comet Assay as a Tool to Detect the Genotoxic Potential of Nanomaterials, Nanomaterials (Basel, Switzerland) 9 (2019).

[23] A. Huk, E. Izak-Nau, B. Reidy, M. Boyles, A. Duschl, I. Lynch, M. Dusinska, Is the toxic potential of nanosilver dependent on its size? Part. Fibre Toxicol. 11 (2014) 65.

[24] M. Dusinska, S. Boland, M. Saunders, L. Juillerat-Jeanneret, L. Tran, G. Pojana, A. Marcomini, K. Volkovova, J. Tulinska, L.E. Knudsen, L. Gombau, M. Whelan, A. R. Collins, F. Marano, C. Housiadas, D. Bilanicova, B. Halamoda Kenzaoui, S. Correia Carreira, Z. Magdolenova, L.M. Fjellsbo, A. Huk, R. Handy, L. Walker, M. Barancokova, A. Bartonova, E. Burello, J. Castell, H. Cowie, M. Drlickova, R. Guadagnini, G. Harris, M. Harju, E.S. Heimstad, M. Hurbankova, A. Kazimirova, Z. Kovacikova, M. Kuricova, A. Liskova, A. Milcamps, E. Neubauerova, T. Palosaari, P. Papazafiri, M. Pilou, M.S. Poulsen, B. Ross, E. Runden-Pran, K. Sebekova, M. Staruchova, D. Vallotto, A. Worth, Towards an alternative testing strategy for nanomaterials used in nanomedicine: lessons from NanoTEST, Nanotoxicology 9 (Suppl 1) (2015) 118–132.

[25] NANoREG, <NANoREG_D5_06_DR_Identification_and_optimization_of_the_most_suitable_in_vitro_methodology_Yo3qmgPoS9aEh1–9l2OVcA.pdf>, 2016.

[26] NANOGENOTOX, The Generix NANOGENOTOX dispersion protocol-Standard operation Procedure (SOP) and Background Documentation., 2012, pp. DF-1.7 4 0 obj << /Filter /FlateDecode /Length 18623 >> stream xœí}É'¤Jä=¿"Î-â) ,;ð}ê (‘™>DÈöÿ:# ÜÔÌ "—âòYA.

[27] A.R. Collins, M. Dusinska, Oxidation of cellular DNA measured with the comet assay, Methods in molecular biology (Clifton, N.J.), 186 (2002) 147–159.

[28] ECHA, Recommendations for nanomaterials applicable to the Guidance on QSARs and Grouping of Chemicals, 2017.

[29] S. Charles, S. Jomini, V. Fessard, E. Bigorgne-Vizade, C. Rousselle, C. Michel, Assessment of the in vitro genotoxicity of TiO(2) nanoparticles in a regulatory context, Nanotoxicology 12 (2018) 357–374.

[30] SCCS, <sccs_o_238.pdf>, (2020).

[31] G.C. Falck, H.K. Lindberg, S. Suhonen, M. Vippola, E. Vanhala, J. Catalán, K. Savolainen, H. Norppa, Genotoxic effects of nanosized and fine TiO2, Hum. Exp. Toxicol. 28 (2009) 339–352.

[32] S. Murugadoss, F. Brassinne, N. Sebaihi, J. Petry, S.M. Cokic, K.L. Van Landuyt, L. Godderis, J. Mast, D. Lison, P.H. Hoet, S. van den Brule, Agglomeration of titanium dioxide nanoparticles increases toxicological responses in vitro and in vivo, Part. Fibre Toxicol. 17 (2020) 10.

[33] A. Kazimirova, M. Baranokova, M. Staruchova, M. Drlickova, K. Volkovova, M. Dusinska, Titanium dioxide nanoparticles tested for genotoxicity with the comet and micronucleus assays in vitro, ex vivo and in vivo, Mutat. Res. Genet. Toxicol. Environ. Mutagen. 843 (2019) 57–65.

[34] D.M. Brown, P.H. Danielsen, R. Derr, N. Moelijker, P. Fowler, V. Stone, G. Hendriks, P. Møller, A. Kermanizadeh, The mechanism-based toxicity screening of particles with use in the food and nutrition sector via the ToxTracker reporter system, Toxicol. Vitr.: Int. J. Publ. Assoc. BIBRA 61 (2019), 104594.

[35] M. Gea, S. Bonetta, L. Iannarelli, A.M. Giovannozzi, V. Maurino, S. Bonetta, V.-D. Hodoroaba, C. Armato, A.M. Rossi, T. Schilirò, Shape-engineered titanium dioxide nanoparticles (TiO2-NPs): cytotoxicity and genotoxicity in bronchial epithelial cells, Food Chem. Toxicol. 127 (2019) 89–100.

[36] Z. Wang, Q. Li, L. Xu, J. Ma, Y. Wang, B. Wei, W. Wu, S. Liu, Ageing alters the physicochemical properties of silver nanoparticles and consequently compromises their acute toxicity in mammals, Ecotoxicol. Environ. Saf. 196 (2020), 110487.

[37] T. Zaiter, R. Cornu, N. Millot, M. Herbst, Y. Pellequer, G. Moarbess, H. Martin, M. Diab-Assaf, A. Béduneau, Size effect and mucus role on the intestinal toxicity of the E551 food additive and engineered silica nanoparticles, Nanotoxicology 16 (2022) 165–182.

[38] A. Déciga-Alcaraz, E.I. Medina-Reyes, N.L. Delgado-Buenrostro, C. Rodríguez-Ibarra, A. Ganem-Rondero, G.J. Vázquez-Zapién, M.M. Mata-Miranda, J.H. Limón-Pacheco, C.M. García-Cuéllar, Y. Sánchez-Pérez, Y.I. Chirino, Toxicity of engineered nanomaterials with different physicochemical properties and the role of protein corona on cellular uptake and intrinsic ROS production, Toxicology 442 (2020), 152545.

[39] G. Griffiths, J. Gruenberg, M. Marsh, J. Wohlmann, A.T. Jones, R.G. Parton, Nanoparticle entry into cells; the cell biology weak link, Adv. Drug Deliv. Rev. 188 (2022), 114403.

[40] N. Oh, J.H. Park, Endocytosis and exocytosis of nanoparticles in mammalian cells, Int. J. Nanomed. 9 (Suppl 1) (2014) 51–63.

[41] A. Yang, J. Wu, C. Deng, T. Wang, P. Bian, Genotoxicity of zinc oxide nanoparticles in plants demonstrated using transgenic arabidopsis thaliana, Bull. Environ. Contam. Toxicol. 101 (2018) 514–520.

[42] S. Zhang, H. Gao, G. Bao, Physical principles of nanoparticle cellular endocytosis, ACS nano 9 (2015) 8655–8671.

[43] J. Mosquera, I. García, L.M. Liz-Marzán, Cellular uptake of nanoparticles versus small molecules: a matter of size, Acc. Chem. Res. 51 (2018) 2305–2313.

[44] P.O. Andersson, C. Lejon, B. Ekstrand-Hammarström, C. Akfur, L. Ahlinder, A. Bucht, L. Osterlund, Polymorph- and size-dependent uptake and toxicity of TiO_2 nanoparticles in living lung epithelial cells, Small 7 (2011) 514–523.

[45] L. Shang, K. Nienhaus, G.U. Nienhaus, Engineered nanoparticles interacting with cells: size matters, J. Nanobiotechnol. 12 (2014) 5.

[46] P. Jalili, B.-C. Krause, R. Lanceleur, A. Burel, H. Jungnickel, A. Lampen, P. Laux, A. Luch, V. Fessard, K. Hogeveen, Chronic effects of two rutile TiO2 nanomaterials in human intestinal and hepatic cell lines, Part. Fibre Toxicol. 19 (2022) 37.

[47] M.L. Jugan, S. Barillet, A. Simon-Deckers, N. Herlin-Boime, S. Sauvaigo, T. Douki, M. Carriere, Titanium dioxide nanoparticles exhibit genotoxicity and impair DNA repair activity in A549 cells, Nanotoxicology 6 (2012) 501–513.

[48] L. Ahlinder, B. Ekstrand-Hammarström, P. Geladi, L. Osterlund, Large uptake of titania and iron oxide nanoparticles in the nucleus of lung epithelial cells as measured by Raman imaging and multivariate classification, Biophys. J. 105 (2013) 310–319.

[49] R.K. Shukla, A. Kumar, D. Gurbani, A.K. Pandey, S. Singh, A. Dhawan, TiO(2) nanoparticles induce oxidative DNA damage and apoptosis in human liver cells, Nanotoxicology 7 (2013) 48–60.

[50] H. Louro, A. Tavares, N. Vital, P.M. Costa, E. Alverca, E. Zwart, W.H. de Jong, V. Fessard, J. Lavinha, M.J. Silva, Integrated approach to the in vivo genotoxic effects of a titanium dioxide nanomaterial using LacZ plasmid-based transgenic mice, Environ. Mol. Mutagen. 55 (2014) 500–509.

[51] A.K. Jain, V.A. Senapati, D. Singh, K. Dubey, R. Maurya, A.K. Pandey, Impact of anatase titanium dioxide nanoparticles on mutagenic and genotoxic response in Chinese hamster lung fibroblast cells (V-79): the role of cellular uptake, Food Chem. Toxicol.: Int. J. Publ. Br. Ind. Biol. Res. Assoc. 105 (2017) 127–139.

[52] S. Bettini, E. Boutet-Robinet, C. Cartier, C. Coméra, E. Gaultier, J. Dupuy, N. Naud, S. Taché, P. Grysan, S. Reguer, N. Thieriet, M. Réfrégiers, D. Thiaudière, J. P. Cravedi, M. Carrière, J.N. Audinot, F.H. Pierre, L. Guzylack-Piriou, E. Houdeau, Food-grade TiO(2) impairs intestinal and systemic immune homeostasis, initiates preneoplastic lesions and promotes aberrant crypt development in the rat colon, Sci. Rep. 7 (2017) 40373.

[53] A. Kazimirova, N. El Yamani, L. Rubio, A. Garcia-Rodriguez, M. Barancokova, R. Marcos, M. Dusinska, Effects of titanium dioxide nanoparticles on the Hprt gene mutations in V79 hamster cells, Nanomaterials 10 (2020).

[54] N. Panté, M. Kann, Nuclear pore complex is able to transport macromolecules with diameters of about 39 nm, Mol. Biol. Cell 13 (2002) 425–434.

[55] L.J. Terry, E.B. Shows, S.R. Wente, Crossing the nuclear envelope: hierarchical regulation of nucleocytoplasmic transport, Science 318 (2007) 1412–1416.

[56] J.A. Kim, C. Åberg, A. Salvati, K.A. Dawson, Role of cell cycle on the cellular uptake and dilution of nanoparticles in a cell population, Nat. Nanotechnol. 7 (2011) 62–68.

[57] S. Wang, L.A. Hunter, Z. Arslan, M.G. Wilkerson, J.K. Wickliffe, Chronic exposure to nanosized, anatase titanium dioxide is not cyto- or genotoxic to Chinese hamster ovary cells, Environ. Mol. Mutagen. 52 (2011) 614–622.

[58] E.C. Demir, Amadeu; Marcos, Ricard, Titanium dioxide and zinc oxide nanoparticles are not mutagenic in the mouse lymphoma assay but modulate the mutagenic effect of uv-c-light post treatment, Fresenius Environ. Bull. 26 (2017) 1001–1016.

[59] Z. Chen, Y. Wang, T. Ba, Y. Li, J. Pu, T. Chen, Y. Song, Y. Gu, Q. Qian, J. Yang, G. Jia, Genotoxic evaluation of titanium dioxide nanoparticles in vivo and in vitro, Toxicol. Lett. 226 (2014) 314–319.

[60] L. Armand, A. Tarantini, D. Beal, M. Biola-Clier, L. Bobyk, S. Sorieul, K. Pernet-Gallay, C. Marie-Desvergne, I. Lynch, N. Herlin-Boime, M. Carriere, Long-term exposure of A549 cells to titanium dioxide nanoparticles induces DNA damage and sensitizes cells towards genotoxic agents, Nanotoxicology 10 (2016) 913–923.

[61] E. Elje, E. Mariussen, O.H. Moriones, N.G. Bastús, V. Puntes, Y. Kohl, M. Dusinska, E. Rundén-Pran, Hepato(Geno)toxicity assessment of nanoparticles in a HepG2 liver spheroid model, Nanomaterials 10 (2020).

[62] Z. Magdolenova, D. Bilanicova, G. Pojana, L.M. Fjellsbo, A. Hudecova, K. Hasplova, A. Marcomini, M. Dusinska, Impact of agglomeration and different dispersions of titanium dioxide nanoparticles on the human related in vitro cytotoxicity and genotoxicity, J. Environ. Monit.: JEM 14 (2012) 455–464.

[63] Y. Guichard, J. Schmit, C. Darne, L. Gaté, M. Goutet, D. Rousset, O. Rastoix, R. Wrobel, O. Witschger, A. Martin, V. Fierro, S. Binet, Cytotoxicity and genotoxicity of nanosized and microsized titanium dioxide and iron oxide particles in Syrian hamster embryo cells, The, Ann. Occup. Hyg. 56 (2012) 631–644.

[64] S.J. Kang, B.M. Kim, Y.J. Lee, H.W. Chung, Titanium dioxide nanoparticles trigger p53-mediated damage response in peripheral blood lymphocytes, Environ. Mol. Mutagen. 49 (2008) 399–405.